Received: 24 April 2021 | Revised: 14 June 2021 | Accepted: 17 June 2021

DOI: 10.1049/nbt2.12065

IET Nanobiotechnology

The Institution of Engineering and Technology WILEY

ORIGINAL RESEARCH PAPER

One-pot synthesis chlorin e6 nano-precipitation for colorectal cancer treatment Ce6 NPs for colorectal cancer treatment

Zhongxing Miao[1] | Yujie Wang[1] | Shengjie Li[1] | Min Zhang[2] | Meng Xu[2]

[1]Department of Gastroenterology Surgery, Dalian Municipal Central Hospital, Dalian, Liaoning, China

[2]Department of Department of Anorectal Surgery, Dalian Municipal Central Hospital, Dalian, Liaoning, China

Correspondence

Meng Xu, Department of Department of Anorectal Surgery, Dalian Municipal Central Hospital, Dalian, Liaoning, 116033, China.
Email: mengxu1981@126.com

Abstract

The drug nanoparticles free of additional carriers hold great promise in drug delivery and are suitable for the therapy of cancers. Herein, we developed a one-pot method to prepare chlorin e6 (Ce6) nano-precipitations (Ce6 NPs) for effective photodynamic therapy of colorectal cancer. The drug loading of Ce6 NPs was around 81% and showed acceptable stability, high biocompatibility as well as effective reactive oxygen species (ROS) generation capability. As a result, the Ce6 NPs can produce significantly elevated ROS upon laser irradiations and achieved better anticancer benefits than free Ce6.

1 | INTRODUCTION

The development of nanotechnology in drug delivery has offered a novel and effective way to cure cancer [1, 2]. As a result, nanotechnology-based drug delivery systems (DDS) are becoming one of the most noted fields in cancer treatments [3, 4]. Numerous studies have successfully developed different types of nano-sized DDSs for the treatment of cancers [5–7]. Due to the special enhanced penetration and retention (EPR) effect of tumour tissues, nano-sized DDSs have shown higher drug accumulation than free drugs, which in turn results in better anticancer performance [8–10].

However, it was also noted that most of the current studies employed additional carriers to load the therapeutic drug molecules due to their disadvantages, such as low stability, solubility and targetability [11–13]. Although carriers offer additional advantages to deal with the above-mentioned shortages, they also introduce other concerns, including cytotoxicity, low reproducibility and most importantly, reduced drug-loading content [14–16]. Therefore, it was suggested that drug molecules capable of self-assembly into nanoparticles without the aid of additional carriers might be of great significance to cancer therapy, which not only promotes the drug-loading content to almost 100% but also realizes fast drug release as well as high local drug concentrations to afford better anticancer performance [17, 18].

Photodynamic therapy (PDT) is a recently emerging treatment for cancer management, which kills cancer cells based on the reactive oxygen species (ROS) created by the photosensitizer upon laser irradiations [19, 20]. PDT can realize site-specific cancer treatment by controlling the application site, time and interval of the laser [21, 22]. Moreover, the side effects can be greatly reduced compared with common chemotherapy, as only cytotoxicity is triggered by the laser [23, 24]. However, most of the currently available PDT agents are not suitable to be administered alone due to their innate disadvantages, such as low stability, solubility and targetability [25, 26]. Therefore, nanotechnology is widely considered a promising tool that helps increase the stability and availability of these drugs. In many previous reported articles, PDT agents were loaded into, conjugated to or adsorbed onto DDSs to afford effective PDT for cancers [27–29]. However, carrier-free formulation of these drugs were rarely reported and needs further investigation. Chlorin e6 (Ce6) is a widely adopted photosensitizer for PDT due to its high laser-ROS transfection efficiency and has been widely adopted in many experimental cases [30–32]. In our opinion, the development of carrier-free Ce6 nanoformulations can significantly increase its PDT efficacy and further promot its application in a variety of biomedical fields.

Here in our study, we aim to develop a one-pot method to prepare Ce6 nanoprecipitation to afford carrier-free delivery of

Ce6 for the therapy of the model cell line of colorectal cancer. Polystyrene maleic anhydride (PSMA) was dissolved in DMSO with Ce6 under agitation to obtain clear solution. Afterwards, the mixture was injected into sonicated solution by a one-pot solvent-diffusion method to obtain PSMA-stabilized carrier-free Ce6 nanoprecipitation (Ce6 NPs). The size, stability as well as biocompatibility of this platform was studied and the PDT effect on HT-29 cells and tumour-bearing mice models was also investigated. Using this method, we can easily obtain a well-controlled Ce6 NPs. This is more convenient than previous reported protocol [33] and might be a good alternative that inspires future research studies.

2 | MATERIALS AND METHOD

2.1 | Materials

All the chemical agents were supplied by Sigma-Aldrich unless otherwise stated. The human colorectal cancer cell line HT-29 was provided by ATCC (United States) and cultured in standard condition as previous reported [34]. The HT-29 tumour-bearing mouse model was established using balb/c nude mice (Qinglongshan, Nanjing, China) as previous reported [35].

2.2 | Preparation of Ce6 NPs

Polystyrene maleic anhydride (PSMA) and Ce6 at the weight ratio of 1:4 were dissolved in a glass vial to obtain a final drug concentration of 2 mg/ml. Afterwards, the mixture was injected into 10-fold of water (v/v) using a syringe under probe-type sonication (VCX2500, Sonics, United States) for 10 min. The final solution's dialysis was performed in a semipermeable membrane (MWCO: 3000 Da) against pure water for 12 h to remove organic solvent and unreacted materials [36].

2.3 | Characterizations

The size of Ce6 NPs (0.1 mg/ml) was measured by Zetasizer Advance (Malvern Panalytical, United Kingdom). The morphology of Ce6 NPs was observed by using a transmission electron microscope (TEM, JEM-1200, JEOL, Japan). The ROS generation of free Ce6 and Ce6 NPs was determined using 3-diphenylisobenzofuran (DPBF) as the probe, according to a previous report [37] DPBF was added into the solution-free Ce6 and Ce6 NPs (final concentration: 10 μg/ml) and then irradiated by using a 680-nm laser (0.2 W/cm^2, 5 min); the changes in absorption at 413 nm was recorded every 30 s. The stability and haemolysis assays were conducted using previous reported protocol [38]. The size of Ce6 NPs in PBS (pH 7.4) and 10% mouse plasma was monitored for 48 h. 2% red blood cells from a rabbit were incubated with Ce6 NPs at different concentrations in the dark for 1 h. In the end, the cells were removed by centrifugation (1500 rpm, 10 min) and the absorption at 413 nm was assessed in comparison to cells treated with pure water.

2.4 | In vitro cellular ROS level and anticancer assay

The DCFH-DA as an ROS probe was employed for the determination of the in vitro cellular ROS level of HT-29 after it was treated with different samples, as previously reported [39]. Cells were incubated with free Ce6 or Ce6 NPs for 4 h; at the last 0.5 h, the cells were loaded with the DCFH-DA, as instructed by the manufacturer. Afterwards, the cells were irradiated (as mentioned above) and the fluorescence signals in the cells were observed by using a fluorescence microscope. Parallel cells were treated for another 48 h and the final cell viability was determined using the methyl thiazolyl tetrazolium (MTT) assay, as reported previously [40].

2.5 | In vivo anticancer assay

The HT-29 tumour-bearing mice were randomly divided into three groups ($n = 5$). The subjects were administered intravenously with saline, free Ce6 and Ce6 NPs (5 mg/kg Ce6) once every 2 days for 2 weeks. The laser was applied three times 24-h post injection (680 nm, 0.5 W/cm^2 for 5 min). The tumour volume of the subjects was recorded and plotted against time. At last, the tumours were collected and assessed by TUNEL and Ki67staining to study their apoptosis and proliferation profiles.

3 | RESULTS AND DISCUSSION

3.1 | Preparation and characterization of Ce6 NPs

According to previous reports, the NPs under nanoscale range usually have larger surface area and tend to aggregate in a short time [41, 42]. Therefore, the introduction of an additional stabilizer is important. In this study, PSMA, as a commonly adopted stabilizer for nanoprecipitation, is employed to help Ce6 forms stable NPs with the aid of sonication. As shown in Figure 1a, the resulting Ce6 NPs were nano-sized particles, which were largely located at the size range of around 70 nm. Previous reports [43, 44] have shown that nanoparticles of size under 100 nm are suitable for targetting tumour tissues via the EPR effect; therefore, Ce6 NPs is a promising formulation to realize passive tumour targetting. Moreover, TEM was also employed to observe the morphology of the nanoparticles. As shown in Figure 1b, Ce6 NPs were shown as spherical particles under self-assembled state. The boundary was clear and the size distributions were uniform, which is consistent with that reported in Figure 1a. After dialysis, the nanoparticles were dissolved in excess volume of DMSO and the Ce6 content was determined by using an ultraviolet spectrophotometer (405 nm), using the standard curve established by the free Ce6. The results revealed that the drug-loading content was around 81%, which further indicated the carrier-free preparation of NPs [45].

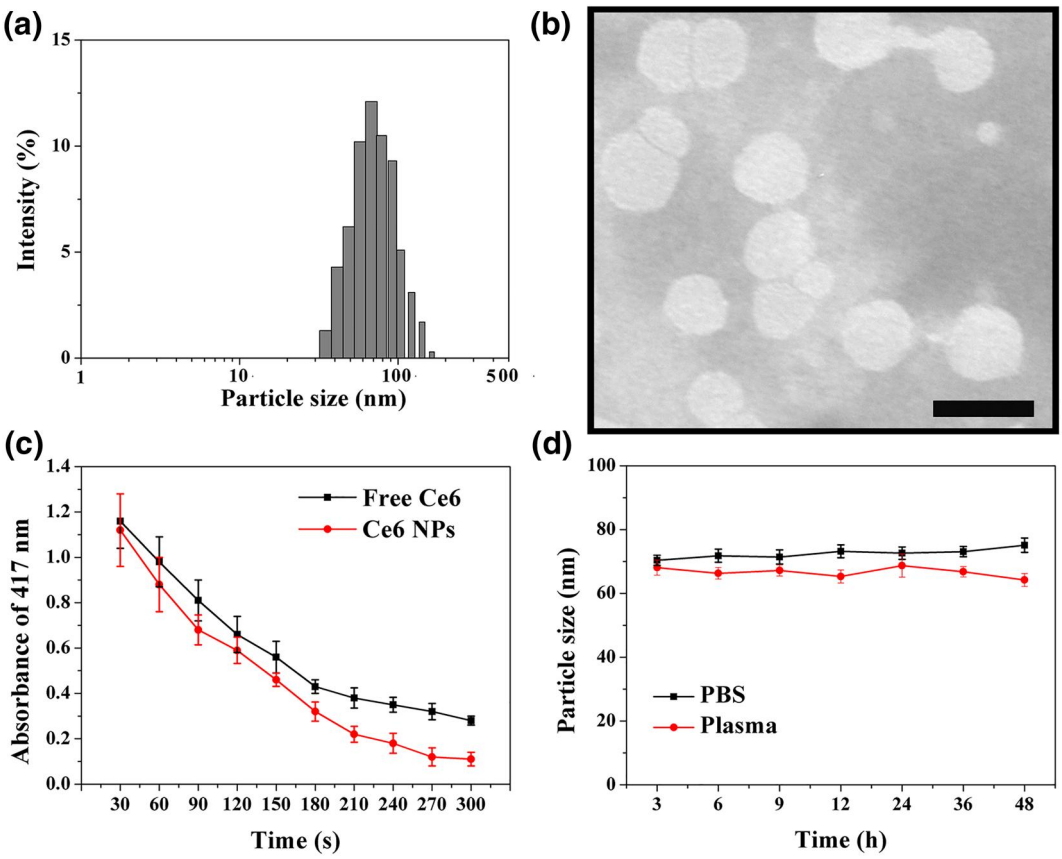

FIGURE 1 Characterization of chlorin e6 nano-precipitations (Ce6 NPs). The size distribution (a) and transmission electron microscope image (b) of Ce6 NPs. Scale bar is 100 nm. The reactive oxygen species generation capability (c) and stability (d) capability of Ce6 NPs. The Ce6 concentration was fixed at 10 μg/ml and the solution was irradiated by 680 nm (0.2 W/cm^2 for 5 min). The results were summarized as average and standard deviation based on three parallel experiments

Afterwards, the ROS generation capacity of Ce6 NPs in comparison with free Ce6 was studied to see if the NPs can still preserve the photodynamic nature of Ce6. As shown in Figure 1c, we used DPBF as the probe whose absorption at 413 nm can be quenched by ROS. Under the same laser irradiation condition, both free Ce6 and Ce6 NPs resulted in significant drop in the absorption (413 nm) of DPBF. Interestingly, it was noted that Ce6 NPs showed faster drop than free Ce6, indicating that the ROS generation by Ce6 NPs is more effective than the ROS generation by free Ce6. According to a previous report, free Ce6 usually suffers from photobleaching and degradation upon laser irradiation [46]. The aggregation state is beneficial to stabilize Ce6 to avoid undesired degradation, which explains the phenomenon that Ce6 NPs had a better ROS generation profile than free Ce6.

In order to further confirm this conclusion, we studied the aqueous stability of Ce6 NPs in two simulated physiological environments, PBS and mouse plasma. As shown in Figure 1d, the size changes of Ce6 NPs were monitored for 48 h to show the stability of Ce6 NPs under physiological environments. It was shown that Ce6 NPs successfully resisted the challenge under both conditions and maintained stability without observable size changes. Therefore, it is expected that Ce6 NPs can bypass the extracellular barriers in a stable form to reach the tumour site and exert PDT on tumours.

Following the confirmation of the stability of Ce6 NPs, the biocompatibility of this platform is another critical issue that needs to be studied. Therefore, haemolysis, as a universal and critical indicator for biocompatibility, is tested. As shown in Figure 2a, series concentrations of Ce6 NPs were incubated with 2% rabbit red blood cells for 1 h and the haemolysis ratio ($OD_{530\ nm}$) was determined. It was observed that the haemolysis of NPs was concentration dependent and the highest concentration of Ce6 NPs (1 mg/ml) only resulted in around 1.75% of haemolysis, indicating that this platform showed no cytotoxicity or irritation on red blood cells. Next, the cytotoxicity of a series concentrations of Ce6 NPs and free Ce6 on HT-29 cells were investigated without laser irradiations for 48 h. As shown in Figure 2b, both free Ce6 and Ce6 NPs showed almost no toxicity on HT-29 cells at all given concentrations for 48 h. This suggested that the toxic effect of Ce6 NPs is controllable through laser irradiation, which is beneficial for reducing the unwanted side effects upon application.

3.2 | In vitro cellular ROS level and anticancer assay

Because the PDT of Ce6-based formulations relies on the generation of ROS, cellular ROS generation is of significant importance to the final anticancer benefits of the formulations. Therefore, the in vitro cellular ROS level was investigated. The cells were first treated with free Ce6 and Ce6 NPs for 4 h and then loaded with the ROS probe DCFH-DA. After replacing the medium with fresh ones, the cells were irradiated by using a 680 nm laser (0.2 W/cm^2 for 5 min) and the intracellular fluorescence was evaluated by flow cytometry (MoFlo Astrios, Beckman, United States). As shown in Figure 3a, in Ce6-treated groups, there was significant elevation of intracellular ROS after laser irradiation, which was in line with previous studies which showed that Ce6 can effectively create ROS upon laser irradiations [47, 48]. Moreover, it was noted that Ce6 NPs had a much higher intracellular ROS level than free Ce6 groups. This result suggested that the accumulation of Ce6 is more powerful in cells using Ce6 NPs than those using free Ce6. A higher cellular ROS level is expected to induce higher cytotoxicity on cells. As a proof of concept, the viability of HT-29 cells subjected to free Ce6 and Ce6 NPs' treatment at different drug concentrations was studied. The cells were incubated with formulations for 4 h and then treated by laser irradiations (680 nm, 0.2 W/cm^2, 5 min). They were incubated for another 24 h and then assessed by MTT assay. As shown in Figure 3b, both free Ce6 and Ce6 NPs showed concentration-dependent increase in cytotoxicity and it was noted that the cell viability in the Ce6 NPs group was lower than that in the free Ce6 group under all tested concentrations.

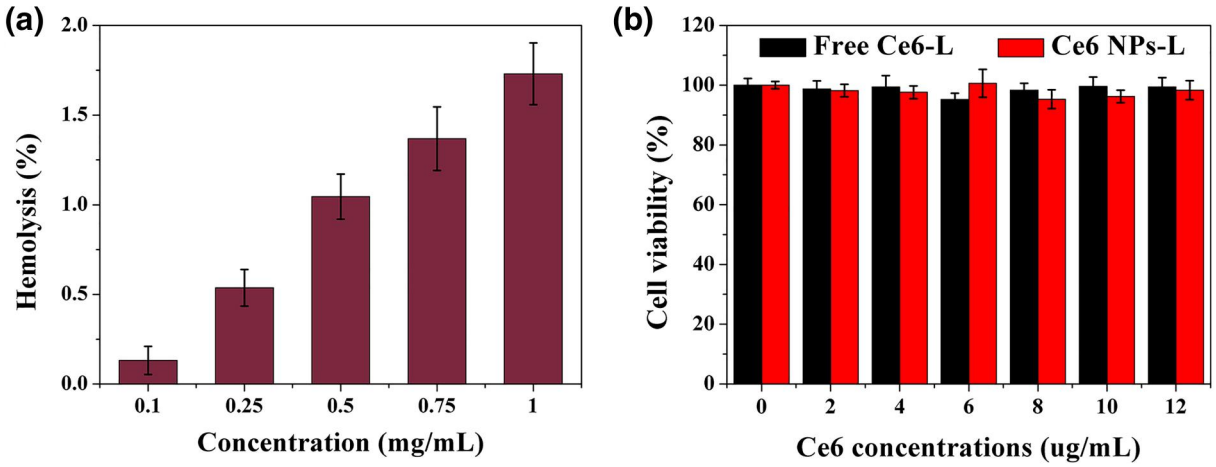

FIGURE 2 Characterization of chlorin e6 nano-precipitations (Ce6 NPs). (a) The haemolysis ratio of 2% rabbit red blood cells in various concentrations of Ce6 NPs for 1 h. (b) The viability of HT-29 cells after incubation with different concentrations of free Ce6 and Ce6 NPs without light for 48 h. The results were summarized as average and standard deviation based on three parallel experiments

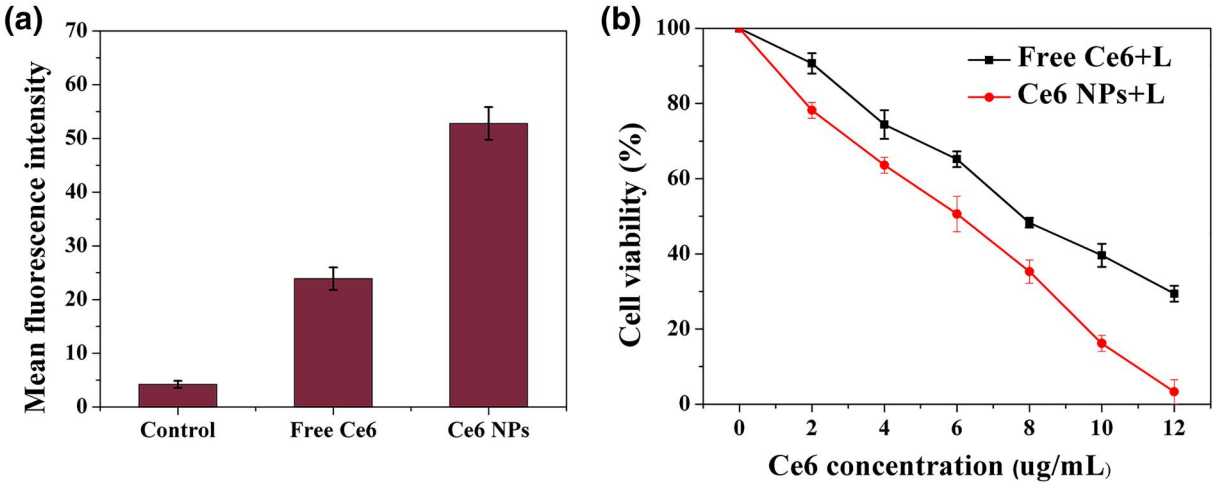

FIGURE 3 (a) Quantitative flow cytometry analysis of intracellular fluorescence intensity, indicating the oxidative stress. (b) Viability of HT-29 cells treated with different formulations at different Ce6 concentrations for 24 h. The results were summarized as average and standard deviation based on three parallel experiments

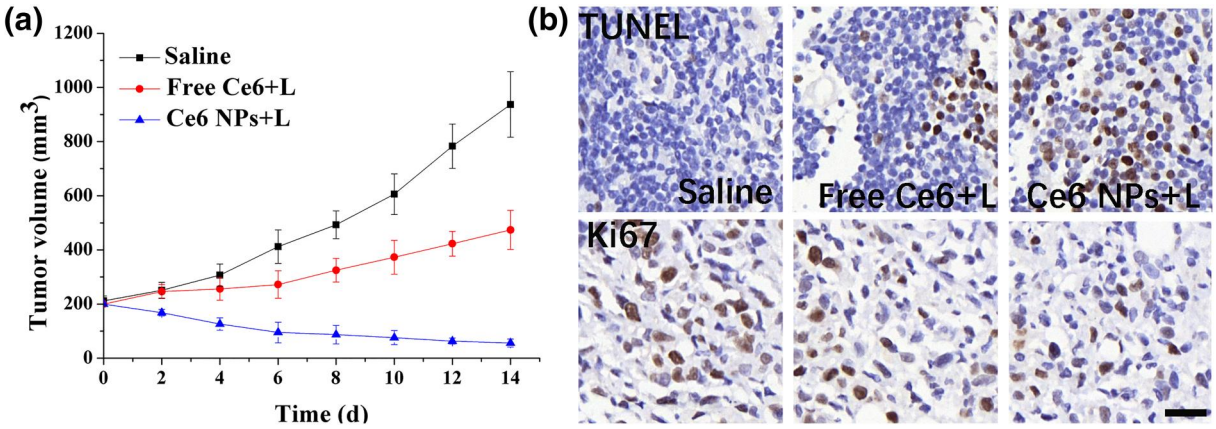

FIGURE 4 (a) The changes in the tumour volume in HT-29-bearing mice treated with different formulations. The Ce6 dosage was 5 mg/kg and all mice were subjected to laser irradiation of 1.5 W/cm^2 for 5 min, 24 h post administration. During the test, variations in the tumour volume were monitored before every administration. (b) The tumour weights of tumours from different groups. (c) The TUNEL and Ki67 staining of tumour tissues obtained from different groups after experiments. Scale bar is 50 μm. The results were summarized as average and standard deviation based on five parallel experiments

3.3 | In vivo anticancer assay

At last, we tested the in vivo anticancer assay to study the extended application of this platform in living samples. The tumour volume was recorded and plotted against time to show the in vivo anticancer benefits. As shown in Figure 4a, compared with the saline group, the laser-treated free Ce6 showed significant decrease in the growth of tumours. But this effect is not powerful enough to cause total tumour remission as the final tumour volume in this group was still over 400 mm^3. As expected, Ce6 NPs showed significantly enhanced anticancer benefits compared to free Ce6, which almost obtained full ablation of tumours at the end of the study. The TUNEL and Ki67 staining also obtained a similar conclusion. As shown in Figure 4b, the tumour tissues that were treated with Ce6 NPs showed serious apoptosis and had the lowest proliferation (brown staining indicated positive cells) compared with the rest of the groups, indicating the best anticancer performance using this platform rather than with free drugs.

4 | CONCLUSION

In summary, we can say that we successfully developed PSMA-stabilized Ce6 NPs as a carrier free platform for PDT for colorectal cancer. The Ce6 NPs showed acceptable stability, high biocompatibility as well as effective ROS generation capability. As a result, we concluded that Ce6 NPs can produce significantly elevated ROS upon laser irradiations and have better anticancer benefits than free Ce6. This strategy provides a facile way of preparing Ce6 NPs, which might be a promising alternative that pushes PDT towards clinical applications.

CONFLICT OF INTEREST

We declare no conflict of interest.

ORCID

Meng Xu https://orcid.org/0000-0002-9470-9410

REFERENCES

1. Goldberg, M.S.: Improving cancer immunotherapy through nanotechnology. Nat. Rev Cancer. 19(10), 587–602 (2019)
2. Cryer, A.M., Thorley, A.J.: Nanotechnology in the diagnosis and treatment of lung cancer. Pharmacol. Therapeut. 198, 189–205 (2019)
3. Kumari, R., Sunil, D., Ningthoujam, R.S.: Hypoxia-responsive nanoparticle based drug delivery systems in cancer therapy: an up-to-date review. J. Contr. Release. 319, 135–156 (2020)
4. Dang, Y., Guan, J.: Nanoparticle-based drug delivery systems for cancer therapy. Smart Mater. Med. 1, 10–19 (2020)
5. Chen, S.-Q., et al.: Quercetin covalently linked lipid nanoparticles: multifaceted killing effect on tumour cells. ACS Omega. 5(46), 30274–-30281 (2020)
6. Wang, C., et al.: Mitoxantrone-preloaded water-responsive phospholipid-amorphous calcium carbonate hybrid nanoparticles for targeted and effective cancer therapy. Int. J. Nanomed. 14, 1503–1517 (2019)
7. Xiong, H., et al.: Self-assembled nano-activator constructed ferroptosis-immunotherapy through hijacking endogenous iron to intracellular positive feedback loop. J. Contr Release. 332, 539–552 (2021)
8. Wang, C., et al.: Size-controlled preparation and behavior study of phospholipid–calcium carbonate hybrid nanoparticles. Int. J. Nanomed. 15, 4049–4062 (2020)
9. Ji, C., et al.: Activatable photodynamic therapy for prostate cancer by NIR dye/photosensitizer loaded albumin nanoparticles. J. Biomed. Nanotechnol. 15(2), 311–318 (2019)
10. Aghebati-Maleki, A., et al.: Nanoparticles and cancer therapy: perspectives for application of nanoparticles in the treatment of cancers. J. Cell. Physiol. 235(3), 1962–72 (2020)
11. Khalifa, A.M., et al.: Current strategies for different paclitaxel-loaded nano-delivery systems towards therapeutic applications for ovarian carcinoma: a review article. J. Contr. Release. 311, 125–137 (2019)
12. Uz, M., Alsoy Altinkaya, S., Mallapragada, S.K.: Stimuli responsive polymer-based strategies for polynucleotide delivery. J. Mater. Res. 32(15), 2930–2953 (2017)
13. Chen, R., et al.: A photoacoustic shockwave triggers the size shrinkage of nanoparticles to obviously improve tumour penetration and therapeutic efficacy. Nanoscale. 11(3), 1423–1436 (2019)
14. Wang, M., et al.: Recent advances in glucose-oxidase-based nanocomposites for tumor therapy. Small. 15(51), 1903895 (2019)

15. Zhang, Z., et al.: Holo-lactoferrin modified liposome for relieving tumour hypoxia and enhancing radiochemotherapy of cancer. Small. 15(6), 1803703 (2019)
16. Liu, W., et al.: Self-activated in vivo therapeutic cascade of erythrocyte membrane-cloaked iron-mineralized enzymes. Theranostics. 10(5), 2201–2214 (2020)
17. Sheokand, S., Navik, U., Bansal, A.K.: Nanocrystalline solid dispersions (NSD) of hesperetin (HRN) for prevention of 7, 12-dimethylbenz [a] anthracene (DMBA)-induced breast cancer in Sprague-Dawley (SD) rats. Eur. J. Pharmaceut. Sci. 128, 240–249 (2019)
18. Dev, A., et al.: Paclitaxel nanocrystalline assemblies as a potential transcatheter arterial chemoembolization (TACE) candidate for unresectable hepatocellular carcinoma. Mater. Sci. Eng. C. 107, 110315 (2020)
19. Wang, C., et al.: Dual-channel theranostic system for quantitative self-indication and low-temperature synergistic therapy of cancer. Small. 17(10), 2007953 (2021)
20. Shi, X., et al.: Recent advances in photodynamic therapy for cancer and infectious diseases. Wiley Interdiscip. Rev. Nanomed. Nanobiotechnol. 11(5), e1560 (2019)
21. Banerjee, S.M., et al.: Photodynamic therapy in primary breast cancer. J. Clin. Med. 9(2), 483 (2020)
22. Mansoori, B., et al.: Photodynamic therapy for cancer: role of natural products. Photodiagnosis Photodyn. Ther. 26, 395–404 (2019)
23. McFarland, S.A., et al.: Metal-based photosensitizers for photodynamic therapy: the future of multimodal oncology? Curr. Opin. Chem. Biol. 56, 23–27 (2020)
24. Curcio, A., et al.: Iron oxide nanoflowers@ CuS hybrids for cancer tri-therapy: interplay of photothermal therapy, magnetic hyperthermia and photodynamic therapy. Theranostics. 9(5), 1288–1302 (2019)
25. Song, Y., Wang, L., Xie, Z.: Metal–organic frameworks for photodynamic therapy: emerging synergistic cancer therapy. Biotechnol. J. 16, 1900382 (2020)
26. Wang, Y., et al.: Sequentially self-assembled polysaccharide-based nanocomplexes for combined chemotherapy and photodynamic therapy of breast cancer. Carbohydr. Polym. 203, 203–213 (2019)
27. Fan, N., et al.: ALP-activated chemiluminescence PDT nano-platform for liver cancer-specific theranostics. ACS Appl. Bio Mater. 4(2), 1740–1748 (2021)
28. Sui, C., et al.: MOFs-derived Fe–N codoped carbon nanoparticles as O_2-evolving reactor and ROS generator for CDT/PDT/PTT synergistic treatment of tumors. Bioconjug. Chem. 32(2), 318–327 (2021)
29. Zhang, Y., et al.: Multifunctional nanoparticles as photosensitizer delivery carriers for enhanced photodynamic cancer therapy. Mater. Sci. Eng. C. 115, 111099 (2020)
30. Cheng, X., et al.: Oxygen-producing catalase-based prodrug nanoparticles overcoming resistance in hypoxia-mediated chemo-photodynamic therapy. Acta Biomater. 112, 234–249 (2020)
31. Zhao, X., et al.: Chitosan derived glycolipid nanoparticles for magnetic resonance imaging guided photodynamic therapy of cancer. Carbohydr. Polym. 245, 116509 (2020)
32. Feng, J., et al.: Stem cell membrane–camouflaged bioinspired nanoparticles for targeted photodynamic therapy of lung cancer. J. Nanoparticle Res. 22(7), 1–11 (2020)
33. Liu, Y., et al.: Water-insoluble photosensitizer nanocolloids stabilized by supramolecular interfacial assembly towards photodynamic therapy. Sci. Rep. 7(1), 1–8 (2017)
34. Tao, S., et al.: Water/pH dual responsive in situ calcium supplement collaborates simvastatin for osteoblast promotion mediated osteoporosis therapy via oral medication. J. Contr. Release. 329, 121–135 (2021)
35. Wang, H., et al.: Nanoparticles-mediated reoxygenation strategy relieves tumor hypoxia for enhanced cancer therapy. J. Contr. Release. 319, 25–45 (2020)
36. Wang, Z., et al.: Donor–acceptor-type conjugated polymer-based multi-coloured drug carriers with tunable aggregation-induced emission behavior for self-illuminating cancer therapy. ACS Appl. Mater. Interfaces. 11(45), 41853–41861 (2019)
37. Borodziuk, A., et al.: Unmodified Rose Bengal photosensitizer conjugated with NaYF4:Yb, Er upconverting nanoparticles for efficient photodynamic therapy. Nanotechnology. 31(46), 465101 (2020)
38. Sun, Y., et al.: Facile preparation of cancer cell membrane vehicle loaded with indocyanine green for effective photothermal therapy of cancer. Micro & Nano Lett. 15(11), 784–787 (2020)
39. Yang, J., et al.: Pseudomonas aeruginosa synthesized silver nanoparticles inhibit cell proliferation and induce ROS mediated apoptosis in thyroid cancer cell line (TPC1). Artif. Cells Nanomed. Biotechnol. 48(1), 800–809 (2020)
40. Roggia, I., et al.: Protective effect of guarana-loaded liposomes on hemolytic activity. Colloids Surf. B Biointerfaces. 187, 110636 (2020)
41. Dou, J., et al.: Preparation of non-spherical vaterite $CaCO_3$ particles by flash nano precipitation technique for targeted and extended drug delivery. J. Drug Deliv. Sci. Technol. 57, 101768 (2020)
42. Jadon, R.S., Sharma, M.: Docetaxel-loaded lipid-polymer hybrid nanoparticles for breast cancer therapeutics. J. Drug Deliv. Sci. Technol. 51, 475–484 (2019)
43. Kang, J.H., Cho, J., Ko, Y.T.: Investigation on the effect of nanoparticle size on the blood–brain tumour barrier permeability by in situ perfusion via internal carotid artery in mice. J. Drug Target. 27(1), 103–110 (2019)
44. Peng, J., Liang, X.: Progress in research on gold nanoparticles in cancer management. Medicine. 98(18) (2019)
45. Zhang, X., et al.: Cetuximab-modified silica nanoparticle loaded with ICG for tumor-targeted combinational therapy of breast cancer. Drug Deliv. 26(1), 129–136 (2019)
46. Liu, Y., et al.: Near-infrared light-triggered nanobomb for in situ on-demand maximization of photothermal/photodynamic efficacy for cancer therapy. Biomater. Sci. 9(3), 700–711 (2021)
47. Sun, X., et al.: Ce6-C6-TPZ co-loaded albumin nanoparticles for synergistic combined PDT-chemotherapy of cancer. J. Mater. Chem. B. 7(38), 5797–5807 (2019)
48. Duan, M., et al.: Matrix metalloproteinase-2-targeted superparamagnetic Fe_3O_4-PEG-G5-MMP2@Ce6 nanoprobes for dual-mode imaging and photodynamic therapy. Nanoscale. 11(39), 18426–18435 (2019)

How to cite this article: Miao, Z., et al.: One-pot synthesis chlorin e6 nano-precipitation for colorectal cancer treatment Ce6 NPs for colorectal cancer treatment. IET Nanobiotechnol. 15(8), 680–685 (2021). https://doi.org/10.1049/nbt2.12065